



Response of E-glass/vinyl ester composite panels to underwater explosive loading: Effects of laminate modifications

James LeBlanc^{a,*}, Arun Shukla^b

^aNaval Undersea Warfare Center (Division Newport), 1176 Howell Street, Newport, RI 02841, USA

^bUniversity of Rhode Island, 92 Upper College Road, Kingston, RI 02881, USA

ARTICLE INFO

Article history:

Received 25 March 2011

Received in revised form

3 May 2011

Accepted 5 May 2011

Available online 13 May 2011

Keywords:

Composite damage

Shock loading

Blast loading

Underwater explosion

Polyurea

ABSTRACT

The response of E-Glass/Vinyl ester curved composite panels subjected to underwater explosive loading has been studied. Three laminate constructions have been investigated to determine their relative performance when subjected to shock loading. These constructions are: (1) a baseline 0°/90° biaxial layup, (2) a 0°/90° biaxial layup that includes a thin glass veil between plies, and (3) a 0°/90° biaxial layup that has a coating of polyurea applied to the back face. The work consists of experimental work utilizing a water filled, conical shock tube facility. The samples are round panels with curved midsections, and are approximately 2.54 mm in thickness. The transient response of the plates is measured using a three-dimensional (3D) Digital Image Correlation (DIC) system, including high speed photography. This ultra high speed system records full field shape and displacement profiles in real time. The results show that the performance of the baseline laminate is improved when coated with the polyurea material, but conversely, is degraded by the inclusion of the glass veils between plies.

Published by Elsevier Ltd.

1. Introduction

Composite materials have been widely used in a variety of applications in the marine, automotive, and transportation industries. These materials offer the advantages of high strength to weight ratios, reduced maintenance costs, and improved corrosion resistance. Recently, there has been an increased interest in composite materials for use in military applications including land vehicles (structural components and armor solutions), advanced ship hull designs, and submarine components. The use of these materials in wartime environments requires that they not only be able to withstand the loads produced by everyday use but also those imparted from explosions and high speed projectile impact. Currently, the response of these materials at static and quasi-static loading rates is well established. However, the response at the high strain rates that shock and ballistic events can induce is not well understood. This leads to an inherent conservative approach to be taken when these structures are designed and constructed. Typically this results in structures which do not fully realize the weight savings afforded by these materials. The focus of the current research is on the response of composite materials subjected to underwater explosions, UNDEX.

* Corresponding author. Tel.: +1 401 832 7920; fax: +1 401 832 7207.

E-mail address: JAMES.M.LEBLANC@Navy.mil (J. LeBlanc).

There are several experimental methodologies used to impart shock loading conditions to structures including explosives, shock tubes, and impulse loading apparatuses. Although the use of explosives offers an ease of use, there are associated deficiencies such as spherical wave fronts and pressure signatures which are often spatially complex and difficult to capture. Shock tubes offer the advantage of plane wave fronts and wave parameters that are easily controlled and repeated. Recently, Espinosa et al. [1] developed a methodology to develop underwater shock conditions through the use of a flyer plate impact and a water filled chamber. The current study utilizes a water filled, conical shock tube that replicates the free field pressure wave expansion of an underwater explosion.

The response of materials subjected to shock and impact loading has been studied over a wide range of loading rates. The effect of shock loading on stainless steel plates subjected to underwater impulsive loads has been presented by Espinosa et al. [1]. Nurick et al. [2,3] have studied the effects of boundary conditions on plates subjected to blast loading and identified distinct failure modes depending on the magnitude of the impulse and standoff. The response of E-Glass and Carbon based composite laminates under shock and explosive loading (including the effects of heat generation during combustion) has been presented by Tekalur et al. [4]. Mouritz [5] studied the effectiveness of adding a light weight, through thickness stitching material to increase the damage

resistance of composites. LeBlanc et al. [6] have studied the effects of shock loading on three-dimensional woven composite materials. Recently, there has been an increased interest in the study of the effect of shock loading on sandwich structures. These studies include the effects of shock and impact loading conditions (Jackson et al. [7], Schubel et al. [8], Arora et al. [9]).

The use of polyurea materials to enhance the failure resistance of materials subjected to explosive loading has become a topic of interest. Polyurea is a synthetic, high strength/high elongation coating that is typically spray cast onto existing structures to increase their resistance to shock and ballistic/shrapnel loading events such as those of a bomb blast. The armed forces have begun to investigate the suitability of these materials for use on military and naval vehicles such as Humvees, troop carriers and ship hulls, Hodge [10]. Research efforts have focused on the use of polyurea coatings on steel plates, composite plates, and as inner layers of sandwich composites. Amini et al. [11–13] have studied the effects of monolithic and polyurea coated steel plates subjected to impulsive loads and showed that polyurea has a positive damage mitigation effect when applied to the back face of the material. They also found that polyurea can enhance the loading and damage levels if applied on the impact side of the plates. In this study it was shown that coating the front face of the panels with the polyurea increased the amount of impact energy transmitted to the plate as compared to when the back face was coated. Gardner et al. [14] studied the effect of polyurea in sandwich composites. It was observed that when a layer of polyurea is placed between the foam core and the back face of the sandwich the blast resistance is improved, while conversely if the polyurea is placed between the front face and the foam core the performance is degraded.

2. Composite material

Three composite material constructions are utilized in this study: (1) 0°/90° biaxial layup, (2) 0°/90° biaxial layup with a glass veil between plies, and (3) 0°/90° biaxial layup with a coating of polyurea. All of the composite material in the study is E-Glass/Vinyl ester. The panels are manufactured using the vacuum assisted resin transfer molding (VARTM) process with a vinyl ester resin, AOC Hydropel R015-AAG-00. All panels were manufactured by LBI Fiberglass located in Groton, CT.

The baseline laminate (1) is a balanced construction of 0° and 90° continuous fibers with the two layers being stitched together rather than woven. The areal weight of the dry fabric is 0.406 kg/m² (12 oz/yd²). The baseline panels in the study consist of 6 plies of the fabric, with each ply oriented in the same direction, i.e. the 0° fibers

Table 1
Thickness and areal weight of laminates.

	Thickness, mm (in)	Areal weight, kg/m ²
0°/90° Baseline laminate	2.54 (0.10)	4.25 (126)
0°/90° With inter-laminar veils	2.54 (0.10)	4.32 (128)
0°/90° Baseline with polyurea	6.6 (0.26)	8.31 (246)

in each ply are parallel. The finished part has a thickness of 2.54 mm (0.10 in.), areal weight of 4.25 kg/m² (126 oz/yd²), and a fiber content of 63% by weight.

The second laminate (2) which is studied is a modified version of the baseline (1). This layup includes the addition of a light weight glass veil in between layers of the 0°/90° fabric. The addition of the glass veil layers would have increased the overall part thickness and areal density, so in an effort to maintain these parameters only 5 layers of the 0°/90° fabric, and correspondingly 4 layers of the veil are utilized in these parts. This laminate is meant to aid in the understanding of what the best laminate choice is (when shock is a concern) if part thickness and areal weight are concerns. The dry glass veil has an areal weight of 0.054 kg/m² (1.62 oz/yd²). The finished part has a thickness of 2.54 mm (0.10 in.), areal weight of 4.32 kg/m² (128 oz/yd²), and a fiber content of 60% by weight. This construction is being investigated because although fiberglass cloths of continuous, oriented fibers have high in-plane strengths when the fibers are oriented in the loading direction, they can suffer from low through thickness strength, meaning they are susceptible to delamination damage. The incorporation of a glass veil of chopped fibers is meant to serve as a resin rich layer to improve the inter-laminar strength of the laminates. The practice of alternating plies of fiberglass cloth and chopped strand mats has historically been used in the boat building industry [15,16]. This practice is common enough that many manufactures of fiberglass reinforcing fabrics make products which are combinations of continuous unidirectional fibers with a chopped mat/veil backing.

The final laminate construction (3) utilized in this study is identical to the baseline laminate; however the back face of the panel is coated with polyurea. This laminate is chosen to represent what would typically be found in a real world application where structures are retrofitted (spray coated) with this material as opposed to being incorporated into the original design (Hodge [10]). The polyurea material is applied to the composite panel after manufacturing and is not part of the infusion process. A 4 mm (0.160 in.) thick layer of the material is applied to the back face (concave) of the panels resulting in a total part thickness of 6.6 mm (0.26 in.) and an areal weight of 8.31 kg/m² (246 oz/yd²). It is noted

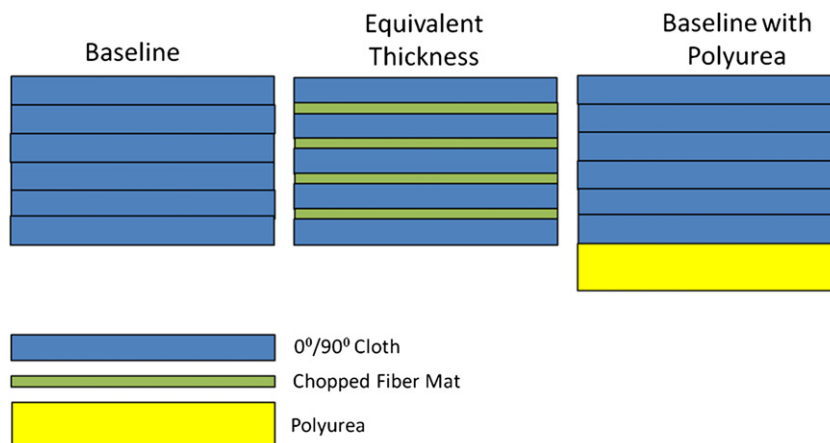


Fig. 1. Composite plate construction – schematic.

Table 2
0°/90° Baseline laminate – mechanical properties (ASTM 638).

	Mpa (lb/in ²)
Tensile modulus (0°)	15.8e3 (2.3e6)
Tensile modulus (90°)	15.8e3 (2.3e6)
Tensile strength (0°)	324 (47,000)
Tensile strength (90°)	324 (47,000)

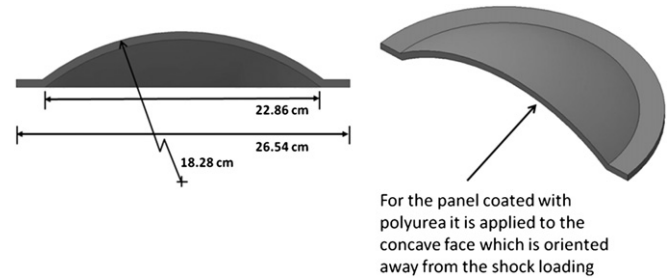


Fig. 2. Composite plate geometry (section view).

that although the total areal weight of this configuration is higher than the baseline panel, the areal weight of the underlying composite itself is equivalent to the baseline composite. The polyurea is sprayed on the panels and then post cured for 48 h at a temperature of 160 °F. In the current study the polyurea is only applied to the back face of the composite panels. This location is chosen based on the prior work by Amini et al. [11–13] and Gardner et al. [14]. These studies have shown that applying the polyurea layer on the back face of shock loaded panels and sandwich composites results in improved performance while, locating the material on the front face can degrade performance.

The polyurea material that is used for coating the panels is Dragonshield-BC available from Specialty Products, Inc. of Lakewood, WA. This is a 2 part material that can be spray applied to a wide range of surface materials. The product is typically used for blast mitigation and fragment containment in applications ranging from walls, structures, and vehicle protection. The manufacturer provides a tensile strength of over 37.9 MPa (5500 lb/in²) and an elongation of 344%.

A summary of the panel thicknesses and areal weights is provided in Table 1, and a schematic of the laminate designs are shown in Fig. 1. The mechanical properties for the 0°/90° baseline and 0°/90° laminate with glass veil inter-laminar plies are provided in Tables 2 and 3. Comparing the values in these tables it is seen that the introduction of the glass veils between plies reduces the in-plane tensile modulus and strengths by 35% and 34% respectively.

The geometry of the plates consists of a curved midsection with a flat boundary as shown in Fig. 2. The convex face of the plate represents the mold line in the manufacturing process and has a radius of curvature of 18.28 cm (7.2 in.), an outer diameter of 26.54 cm (10.45 in.), and the curved portion of the plate is 22.86 cm (9 in.) in diameter.

3. Shock loading apparatus

A conical shock tube (CST) facility located at the Naval Undersea Warfare Center, Division Newport was utilized in the shock loading of the composite materials. The shock tube is a horizontally mounted, water filled tube with a conical internal shape, Fig. 3. The tube geometry represents a solid angle segment of the pressure field that results from the detonation of a spherical, explosive charge, Fig. 4. In an open water environment the pressure wave expands from the charge location as a spherical wave. In the shock tube the rigid wall acts to confine the expansion of the pressure wave in a manner that simulates a conical sector of the pressure field. In order to compare free field and shock tube pressure values, it is useful to define an amplification factor which is the ratio

between the volume of a spherical charge to the volume of the conical sector charge and is defined by Poche and Zalesak [17] as:

$$AF = \frac{1}{\sin^2\left(\frac{\alpha}{4}\right)}$$

α is the cone angle.

This equation assumes perfectly rigid wall conditions which are not fully realized. Therefore, the actual amplification factor is less than the calculated value and is typically reported as an effective weight amplification factor. This is defined by Poche and Zalesak [17] as the ratio between the weight of a spherical charge, W , required to produce the same peak pressure at a given standoff distance as that produced in the shock tube by a segment of charge weight, w . The reduction in the amplification factor is typically attributable to elastic deformation of the shock tube walls. Further discussion on the development and history of the water filled conical shock tube is provided by references [18] and [19].

The internal cone angle of the tube is 2.6°. The tube is 5.25 m (207 in.) long from the charge location to the location of the test specimen and internally contains 98.4 L (26 gal.) of water at atmospheric pressure. The pressure shock wave is initiated by the detonation of an explosive charge at the breech end of the tube (left side of figure) which then proceeds down the length of the tube. Peak shock pressures from 10.3 MPa (1500 lb/in²) to 20.6 MPa (3000 lb/in²) can be obtained depending on the amount of explosive charge. A typical pressure profile obtained from the use of the tube is shown in Fig. 5. This figure illustrates the rapid pressure increase associated with the shock front followed by the exponential decay of the wave. This profile was obtained using a M6 Blasting Cap – 1.32 g (0.00292 lb) TNT Equivalency and is measured 0.508 m (20 in.) from the impact face of the plate. The length of the tube is sufficient so that plane wave conditions are nearly established at the specimen.

A mounting fixture has been designed so the test specimens are air backed with fully clamped edges. The specimens are 26.54 cm (10.45 in.) in overall diameter with a 22.86 cm (9 in.) unsupported middle section. The mounting arrangement is shown in Fig. 6. The specimens are mounted with the convex surface towards the

Table 3
0°/90° Laminate with inter-laminar glass veils – mechanicals properties (ASTM 638).

	Mpa (lb/in ²)
Tensile modulus (0°)	10.3e3 (1.5e6)
Tensile modulus (90°)	10.3e3 (1.5e6)
Tensile strength (0°)	213 (31,000)
Tensile strength (90°)	213 (31,000)

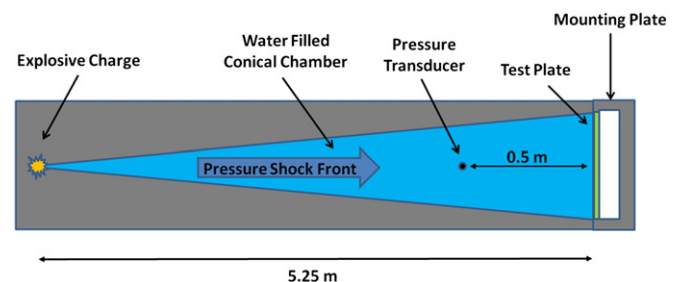


Fig. 3. Conical shock tube schematic (not to scale).

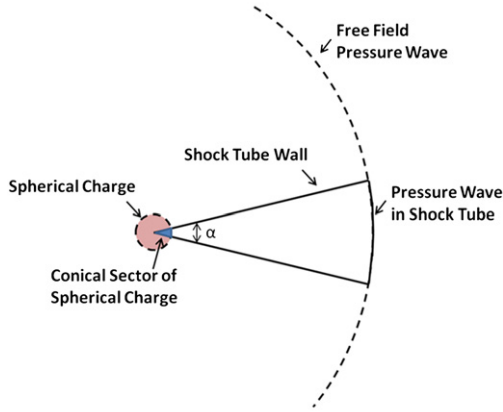


Fig. 4. Explosive charge in shock tube (Poche and Zalesak, 1992).

incoming shock fronts. This is chosen so that the experiment will represent geometries commonly used in underwater applications with curved surfaces typically facing into the fluid (i.e. submersible vehicle hull forms). The radius of curvature of the central part of the plates in this study is a function of the mounting fixture and not representative of a specific structure or vehicle.

4. Experimental procedure

Shock testing of the composite material has been performed with the CST utilizing a fixed end cap. The use of the fixed end cap configuration allows the plate to absorb the full energy level of the shock and sustain a suitable level of damage. The tube can also be configured with a sliding piston end cap (LeBlanc et al. [20]) to lower the level of energy the plate absorbs, but is not utilized in this study. To ensure consistent experiments all shock tests were performed two times and the results were found to be repeatable from test to test. High speed photography coupled with a 3D digital image correlation system is utilized to capture the back face transient response during the shock event. This system offers the advantage that it is a noncontact measurement technique which gives full field information and eliminates the difficulties of strain gages debonding from the specimens at high shock levels and large plate flexures. The explosive charge used in the study is an M6 blasting cap with a net TNT equivalence of 1.32 g. This yields peak pressures at the sensor location (0.508 m in front of the test specimen) of approximately 11 MPa (1600 lb/in²).

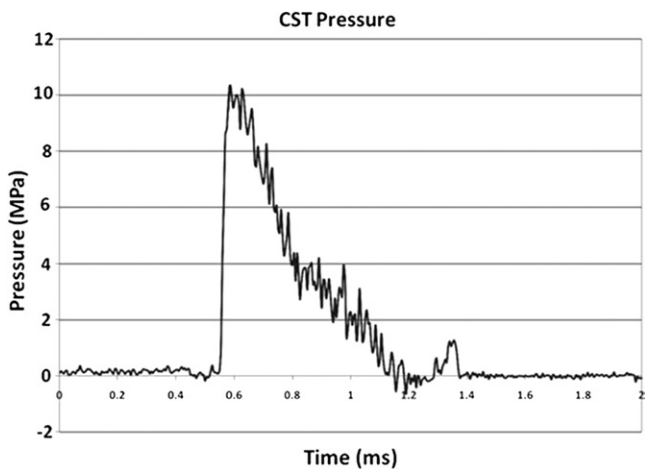


Fig. 5. Typical pressure profile generated in the conical shock tube.

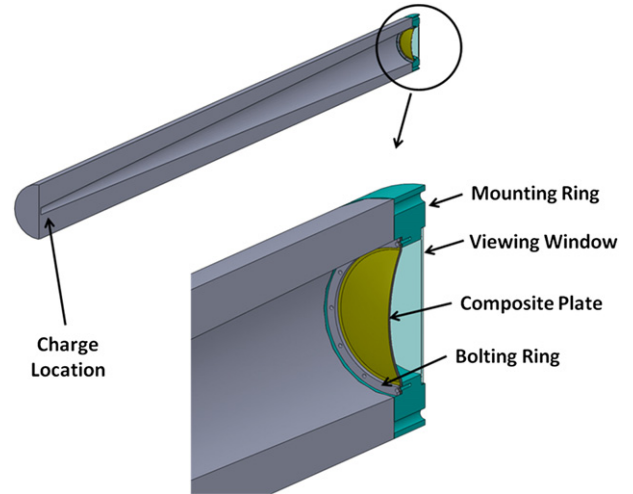


Fig. 6. Shock tube mounting configuration.

The Digital Image Correlation (DIC) technique is used to capture the transient response of the back face (dry) of the plates. DIC is a non-intrusive, optical technique for capturing the full field, transient response of the panels through the use of high speed photography and specialized software. Capturing the three-dimensional response of the plates requires that 2 cameras be used in a stereo configuration. To record the transient response with this system the cameras must be calibrated and have synchronized image recording throughout the event. The calibration of the cameras is performed by placing a grid containing a known pattern of dots in the test space where the composite sample is located during the experiment. This grid is then translated and rotated in and out of plane while manually recording a series of images. As this grid pattern is predetermined, the coordinates of the center of each dot is extracted from each image. The coordinate locations of each dot extracted uniquely for each camera allows for a correspondence of the coordinate system of each camera (Tiwari et al. [21]). The DIC is then performed on the image pairs that are recorded during the shock event. Prior to the experiment, the back face of the sample is painted white and then coated with a randomized speckle pattern, Fig. 7. The post processing is performed with the VIC-3D software package (Correlated Solutions) which matches common pixel subsets of the random speckle pattern between the deformed and un-deformed images. The matching of pixel subsets is used to

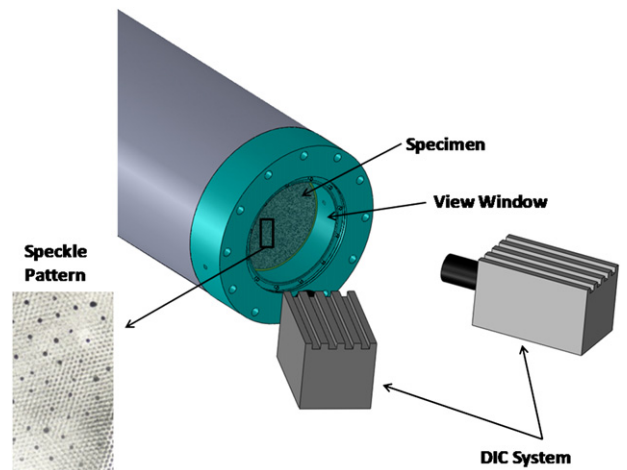


Fig. 7. Digital image correlation schematic.

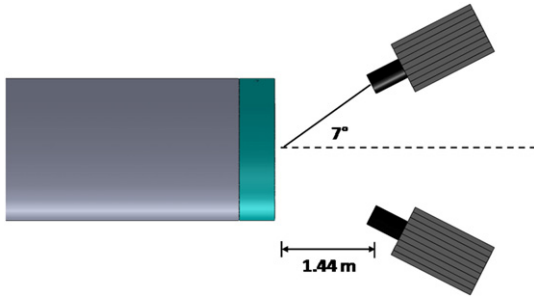


Fig. 8. Digital image correlation setup (not to scale).

calculate the three-dimensional location of distinct points on the face of the panel throughout time. This technique has been applied as a full field measurement technique in many applications including shock loading (Tiwari et al. [22]).

Two high speed digital cameras, Photron SA1, are positioned behind the shock tube, Fig. 7. The use of two cameras allows for the out-of-plane behavior to be captured. If a single camera is utilized the data would be limited to the in-plane results. The distance from the lens of the camera to the specimen is 1.44 m (57 in.) and each camera is angled at approximately 7° with respect to the symmetry plane, Fig. 8. A frame rate of 20,000 was used with an inter-frame time of 50 μs.

5. Results

The determination of the effectiveness of the two laminate modifications in comparison to the baseline laminate will focus on deformation and velocity time histories, as well as the level of post mortem damage. The deformation and velocity histories are presented for distinct points on the back face of the panels, and are extracted from the DIC post processed data. The post mortem damage levels are assessed from visual observations of the damage mechanisms.

The pressure profile obtained from the experiment with the baseline laminate is shown in Fig. 9. The pressure history can be separated into three distinct time regimes. The first is the initial shock front which has time duration of less than 1 ms from peak pressure to full decay to ambient. The second set of pressure effects arrives at the pressure transducer at approximately 10.5 ms after

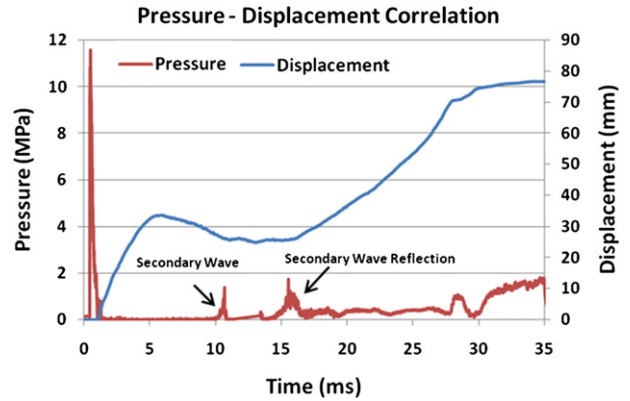


Fig. 9. Pressure – deformation history correlations.

the initial shock front. This secondary wave is formed when the velocity of the plate is brought to rest. During the initial deformation of the plate, the water that contacts the plates moves along with the plate surface. When the movement of the plate is brought to rest, the momentum of this water causes it to compress against the plate and a high pressure wave is developed. This wave then propagates down the length of the tube and is reflected back towards the plate. The time delay from this secondary wave reaching the transducer, traveling down the tube, and arriving back at the transducer is expected to be on the order of 5.5 ms based on the distance of travel from the transducer to the charge location. This time delay is clearly seen in Fig. 9. The bubble pulse for the charge weight and conditions that are used in this study is expected to be on the order of 30 ms, and is confirmed by the high pressures seen in the pressure profiles at this time. From Fig. 10 it is seen that the initial peak pressure for each shot is nearly identical. It is important to note the absence of a reflection of the incident pressure wave in the pressure signal. This is attributable to the similar acoustic impedance values of the water and the composite plate as well as the fluid structure interaction of a plane wave with a curved surface. Consider the case of a dilatation wave arriving at the interface between two dissimilar materials (Water–Composite interface). The wave will be partially transmitted into the plate and partially reflected back into the water. The magnitudes of the reflected (A_2) and transmitted (A_4) waves as a function of the incident wave (A_1) are given by Sadd [23] as:

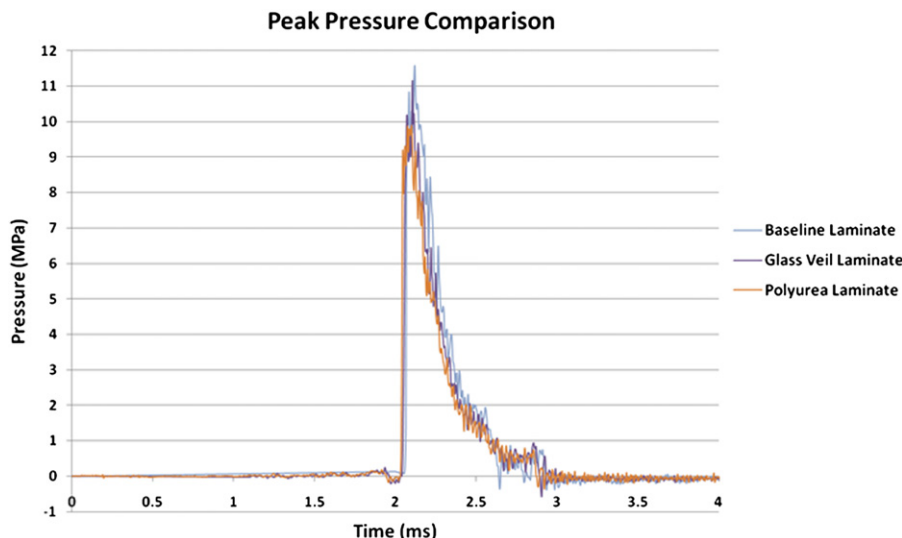


Fig. 10. Pressure profiles (peak pressure comparison) obtained from CST.

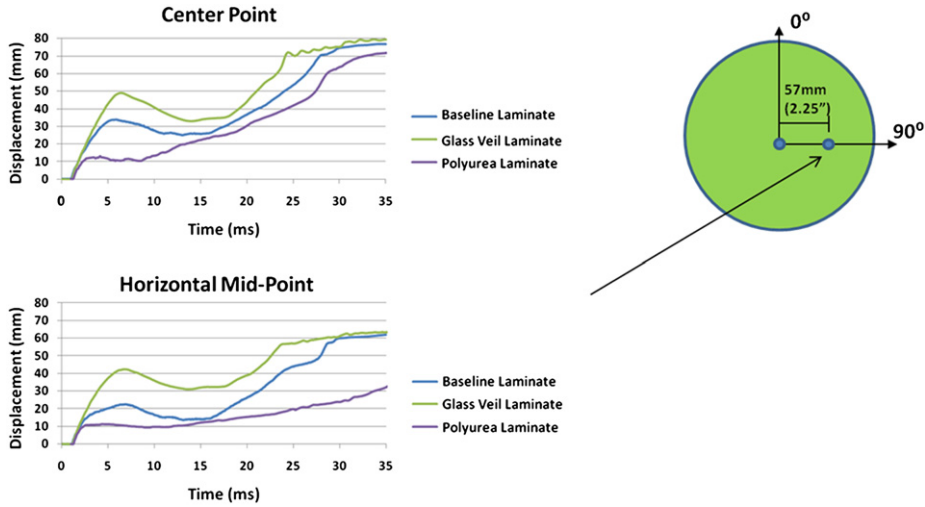


Fig. 11. Time history deformation comparison.

$$A_2 = A_1 - A_4$$

$$A_4 = (A_1 + A_2) \frac{C_{1A}\rho_A}{C_{1B}\rho_B}$$

Where C_1 and ρ are the longitudinal wave speed and the density of the water (A) and the composite (B).

For the water the wave speed and density are 1500 m/s and 1000 kg/m³ and for the composite material the values are 3064 m/s and 1680 kg/m³. These parameters yield a reflected wave magnitude that is 55% of the incident wave. The development of these equations (Sadd, 2009) assume that the surfaces are perfectly bonded with matching of displacements and stresses at the interface. It is likely that these conditions are not fully realized with one of the mediums being water which carries no shear stress, and has the possibility of separating from the composite forming a cavitation region during

the initial deformation of the plate. The development of cavitation at the water/plate interface has been observed by Espinosa et al. (2006) for experiments with steel plates. If perfect matching conditions are not fully realized then the reflected wave has the possibility of further magnitude reduction from the analytical value of 55%. Furthermore, these equations assume a flat interface normal to the incident wave. In the current configuration the wave is interacting with a convexly curved surface which will act to disperse the wave front, further reducing the magnitude of the reflected wave that the pressure transducer would measure. Previous work has observed similar reduced reflection waves. Experiments performed by Espinosa (2006) with steel plates measured reflected waves on the order of 60% of the incident, whereas the theory predicts a value on the order of 95% reflection.

The center point deformation time history along with the corresponding pressure profile for the case of the baseline laminate is shown in Fig. 9. It is seen in this figure that the initial shock causes

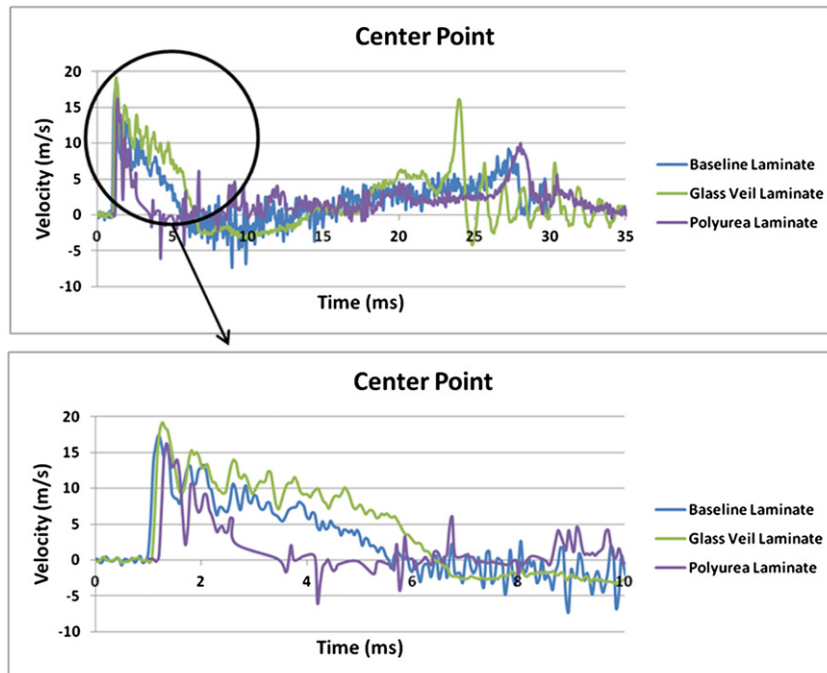


Fig. 12. Velocity history deformation comparison.

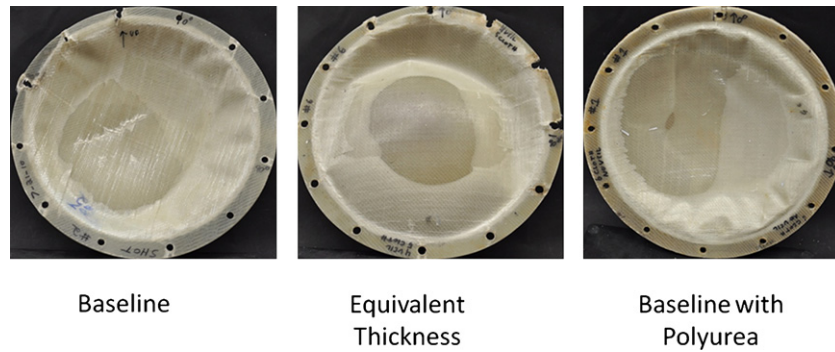


Fig. 13. Material damage comparison.

a deformation of the center point (0–5 ms), a small recovery (5–10 ms), and finally a temporary arresting of the motion (10–15 ms). After this arresting of the motion, the secondary pressure wave arrives (15 ms) and restarts the deformation process of the plate. The effect of the secondary pressure wave is sufficient to carry the deformation process to full inversion of the plate. A similar trend is seen for the other two laminates in this study. A full discussion of the inversion process and associated fluid structure interaction for this composite plate geometry is presented by Leblanc et al. [24].

The comparison of the displacement–time history for the three laminates is shown in Fig. 11. The top plot shows the deflection for the center point and the bottom plot shows the deflection for a point located halfway between the center and the clamped edge along the horizontal axis. Using the baseline laminate as a reference, the panel which is coated with polyurea on the back face shows a distinct performance increase in terms of the displacement sustained after the arrival of the first pressure peak. Conversely, the performance is degraded when glass veil is incorporated between plies but the panel thickness is maintained constant. After the first pressure peak the baseline laminate sustains a center point displacement of 33.5 mm (1.31 in.) while the deflection for the polyurea sample is 11 mm (0.43 in.), a decrease of 67%. In the case of the veil laminate the center point displacement is 48 mm (1.88 in.), an increase of 43% over the baseline. In Table 3 it is shown that the this laminate has a 34% reduction in modulus over the baseline, which likely is the cause for this reduction on deformation behavior, especially since the primary loading mechanism is flexure. In all cases it is seen that the effects of the secondary pressure waves are sufficient to continue the displacement to full plate inversion. This is attributable to the plates being weakened and partially inverted by the initial peak pressure effect.

The velocity time history comparison for the center point of each of the three laminates is shown in Fig. 12. The top plot of this figure shows the velocity history for the total time duration of the event, whereas the bottom plot focuses on the velocity resulting from the initial shock pressure. From the bottom figure it is seen that the magnitude of the kick off velocity for each of the laminates is nearly the same, approximately 16–17 m/s (52.5–55.7 ft/s). There is a difference, however, in the time that it takes for the velocity to decay back to zero for each of the panels. The velocity of the baseline laminate fully decays over 4.5 ms while the panel with polyurea decays faster, taking only 2.4 ms to return to rest. Conversely, the panel with the glass veil layers takes 5.5 ms, 1 ms longer than the baseline panel. An alternative way to compare the decay rate of the velocity is to represent the initial velocity profile as an exponential function as shown below and compute the decay constant, θ , from an exponential curve fit for each panel. The decay

constants respectively for the baseline, polyurea, and the glass veil panels are: -1.9 s, -2.6 s, and -1.0 s.

$$V(t) = V_{\max} e^{\frac{t}{\theta}}$$

The final damage states of the three laminates are shown in Fig. 13. From this figure it is seen that for all of the laminates the primary damage mechanism is delamination, indicated by the lighter regions of the plates. Additionally, each of the panels was sectioned through the center line to ensure that the damage modes were consistent through the thickness. Visual observations indicate that delamination is the primary damage mode not only on the visible external surface but also internal to the plate. There is minimal matrix cracking or fiber breakage observed in any of the panels. There is a small 76.2 mm (3 in.) crack towards the center of the baseline panel but this is limited to the surface of the plate and it does not extend through the thickness of the laminate. It is important to note that these are the final states of damage after the entire shock event occurs, including the secondary deformation process later in time. It was not possible to separate which damage occurs during the initial shock loading and which occurs as a result of the secondary deformation process. Similarly it is not known what the exact damage state after the initial deformation process is and how this initial damage state compares between the three laminates. The only conclusion that can be drawn from these figures is that among the three laminates the final level of damage is comparable, and consists primarily of delamination. This indicates that for these loading conditions and plate geometries, the inclusion of glass veils between plies does not improve the delamination performance of the composite laminate as compared to the baseline.

6. Conclusions

A conical shock tube has been used to study the response of curved E-Glass/Vinyl ester composite panels subjected to underwater shock loading. Three laminate constructions have been investigated and consist of (1) a baseline $0^\circ/90^\circ$ biaxial layup, (2) a $0^\circ/90^\circ$ biaxial layup that includes a thin glass veil between plies, and (3) a $0^\circ/90^\circ$ biaxial layup that has a coating of polyurea applied to the back face. The round plates are curved in shape with the convex surface oriented towards the incoming shock front with fully clamped boundaries. A 3D Digital Image Correlation system is used to capture the full field, transient response of the back (dry) surface of the plates. This allowed for real time recording of the displacement and velocity history of this surface.

The deformation and velocity time histories at several unique points on the back face of the sample are used to evaluate the

effectiveness of each laminate subjected to shock loading conditions. Using the deformation response to the initial peak pressure it was shown that the polyurea reduced the center point deflection by 67%, while the inclusion of glass veils increased the deflection by 43%. In all cases it is seen that the effects of the secondary pressure waves are sufficient to continue the displacement to full plate inversion. It is also observed that the magnitude of the kick off velocity for all panels was the same at around 16 m/s, however the polyurea panel showed the fastest decay of this peak velocity back to zero. Overall damage levels in each of the panels were comparable but it was not possible to separate which damage occurs during the initial shock loading and which occurs as a result of the secondary deformation process. The results show that the performance of the baseline laminate is degraded by the inclusion of the glass veils between plies.

Acknowledgments

The financial support of the Naval Undersea Warfare Center (Division Newport) In-house Laboratory Independent Research program (ILIR) directed by Dr. Anthony Ruffa is greatly acknowledged. Arun Shukla would like to acknowledge the support of Office of Naval Research under ONR Grant No. N00014-10-1-0662 (Dr. Y.D.S. Rajapakse) to the University of Rhode Island. Bruce Booker, Steve Morin, and Jim Sinclair are thanked for their operation of the shock tube facility. The assistance of Nate Gardner, Nicholas Heeder, and Ryan Sekac with the DIC setup is acknowledged. Lastly the authors acknowledge Specialty Products, Inc., specifically Shere Bush, for providing the polyurea material used in this study.

References

- [1] Espinosa HD, Lee S, Moldovan N. A novel fluid structure interaction experiment to investigate deformation of structural elements subjected to impulsive loading. *Exp Mech* 2006;46:805–24.
- [2] Nurick G, Olson M, Fagnan J, Levin A. Deformation and tearing of blast loaded stiffened square plates. *Int J Impact Eng* 1995;16:273–91.
- [3] Nurick G, Shave G. The deformation and tearing of thin square plates subjected to impulsive loads – an experimental study. *Int J Impact Eng* 1996;18:99–116.
- [4] Tekalur AS, Shivakumar K, Shukla A. Mechanical behavior and damage evolution in E-glass vinyl ester and carbon composites subjected to static and blast loads. *Compos Part B Eng* 2008;39:57–65.
- [5] Mouritz AP. Ballistic impact and explosive blast resistance of stitched composites. *Compos. Part B Eng* 2001;32:431–9.
- [6] LeBlanc J, Shukla A, Rousseau C, Bogdanovich A. Shock loading of three-dimensional woven composite materials. *Compos Struct* 2007;79:344–55.
- [7] Jackson M, Shukla A. Performance of sandwich composites subjected to sequential impact and air blast loading. *Compos Part B Eng* 2011;42:155–66. 2010.
- [8] Schubel PM, Luo J, Daniel I. Impact and post impact behavior of composite sandwich panels. *Compos Part A Appl Sci Manuf* 2007;38:1051–7.
- [9] Arora H, Hooper P, Dear JP. Impact and blast resistance of glass fibre reinforced sandwich composite materials. *Proceedings of IMPLAST 2010*. October 2010.
- [10] Hodge N. Military experimenting with 'spray on' armor for humvees. *Defense Today* 2004;25.
- [11] Amini MR, Isaacs JB, Nemat-Nasser S. Experimental investigation of response of monolithic and bilayer plates to impulsive loads. *Int J Impact Eng* 2010;37:82–9.
- [12] Amini MR, Simon J, Nemat-Nasser S. Numerical modeling of effect of polyurea on response of steel plates to impulsive loads in direct pressure-pulse experiments. *Mech Mater* 2010;42:615–27.
- [13] Amini MR, Isaacs JB, Nemat-Nasser S. Investigation of effect of polyurea on response of steel plates to impulsive loads in direct pressure-pulse experiments. *Mech Mater* 2010;42:628–39.
- [14] Gardner N, Wang E, Kumar P, Shukla A. Blast mitigation in a sandwich composite using graded core and polyurea interlayer. *Exp Mech*, in press.
- [15] Geer D. Boat strength for builders, designers, and owners. Fairfield, PA: International Marine, ISBN 0-07-023159-1; 2000.
- [16] Casey D. This old boat. United States of America: International Marine, ISBN 978-0-07-147794-9; 2009.
- [17] Poche L, Zalesak J. Development of a water-filled conical shock tube for shock testing of small sonar transducers by simulation of the test conditions for the heavyweight MIL-S-901D (Navy). *NRL Memorandum Report 7109*; 10 October 1992. Orlando, FL.
- [18] Coombs A, Thornhill CK. An underwater explosive shock gun. *J Fluid Mech* 1967;29:373–83.
- [19] Filler WS. Propagation of shock waves in a hydrodynamic conical shock tube. *Phys Fluids* 1964;7:664–7.
- [20] LeBlanc J, Shukla A. Dynamic response and damage evolution in composite materials subjected to underwater explosive loading: an experimental and computational study. *Compos Struct* 2010;92:2421–30.
- [21] Tiwari V, Sutton MA, McNeill SR. Assessment of high speed imaging systems for 2D and 3D deformation measurements: methodology development and validation. *Exp Mech* 2007;47:561–79.
- [22] Tiwari V, Sutton MA, McNeill SR, Xu S, Deng X, Fournery WL, et al. Application of 3D image correlation for full-field transient plate deformation measurements during blast loading. *Int J Impact Eng* 2009;36:862–74.
- [23] Sadd MH. Wave motion and vibration in continuous media. Kingston, RI: University of Rhode Island; 2009.
- [24] LeBlanc J, Shukla A. Dynamic response of curved composite panels to underwater explosive loading: experimental and computational comparisons. *Compos Struct*, in press, doi:10.1016/j.compstruct.2011.04.017.